

Synthetic Homes: An Accessible Multimodal Pipeline for Producing Residential Building Data with Generative AI

Jackson Eshbaugh
 Department of Computer Science
 Lafayette College
 eshbaugj@lafayette.edu

Chetan Tiwari
 Departments of Computer Science & Geoscience
 Georgia State University
 ctiwari@gsu.edu

Jorge Silveyra
 Department of Computer Science
 Lafayette College
 silveyrj@lafayette.edu

Abstract

Computational models have emerged as powerful tools for multi-scale energy modeling research at the building level as well as urban scale. However, these models require a plethora of data on building parameters, some of which can be inaccessible, expensive, or can raise privacy concerns. We introduce a modular multimodal framework to synthetically produce this data from publicly accessible images and residential information using generative Artificial Intelligence (AI). Additionally, we provide a modeling pipeline demonstrating this framework and we evaluate its generative AI components for realism. Our experiments show that our framework’s use of AI avoids common issues with generative models and produces realistic multimodal data at the building scale. Resulting datasets can be used for assessing influence of energy efficiency upgrades at the building scale, as well as to simulate larger patterns of energy consumption across regions. This work will support research in building and energy simulation by reducing dependence on costly or restricted data sources, and pave a path towards more accessible research in Machine Learning (ML) and other data-driven disciplines.

Keywords: Building Energy Models (BEM), Urban Building Energy Modeling (UBEM), Energy Policy, Synthetic Data, Generative AI

1 Introduction

Consumption of electricity in the United States will increase by 1.7% between 2020 and 2026 (U.S. Energy Information Administration, 2025) and seasonal electricity use per person has nearly doubled from 1973 to 2025 (U.S. Environmental Protection Agency, 2025). Rising energy consumption, due to inefficient building mechanics, exerts increasing pressure on infrastructure capacity, operational costs, and greenhouse gas emissions, resulting in rising costs for governments, energy producers, and energy consumers. Accurate modeling and policy tools are therefore essential for effective planning, aiding by preventing infrastructure strain, optimizing energy costs, minimizing or mitigating climate impacts, assessing policy effectiveness, and guiding decision-making in urban centers (Bompard et al., 2024; Perera et al., 2021; Zeng et al., 2011; Hajri et al., 2025).

Computational approaches—such as the use of Building Energy Models (BEMs) to monitor energy usage and model urban centers, buildings, and other structures—require large amounts of

data, such as type and quality of materials, floor plans, and weather patterns to produce scalable and quantitative results (U.S. Department of Energy). However, several issues arise when attempting to collect such information, including high prices, limited availability, and privacy concerns. These issues create barriers to accessing data, hindering the development of accurate models and the scaling of models to larger populations or geographic areas. The inaccessibility of this data has led researchers to generate synthetic data through a variety of methods. We propose a generative AI based approach to generate low-cost multimodal synthetic data consisting of simulations and home inspection notes that can be used to develop, validate, and improve existing computational models for energy demand modeling. The proposed method enables the generation of large volumes of data for use in any geographic region where basic descriptive data on housing structures is publicly available.

In the following sections, we position our work in the existing literature (Section 2) and provide an in depth view of our framework (Section 3). Then, we evaluate the realism of data generated by our pipeline (Section 4) using a dataset created to statistically model the region of our synthetic homes. Finally we conclude and highlight future directions from this work (Section 5).

2 Related Works

Current data generation efforts span a wide range of approaches, from optimizing building construction processes to the creation of digital twins. For example, Wan et al. (2022) built a generative model that improves the efficiency of energy consumption by determining the optimal layout of floor plans. Elnabawi and Hamza (2022) enhanced their building energy models using highly detailed microclimate models that considered features such as shadow generation and seasons to generate weather data. Lee et al. (2019) train a neural network that predicts building energy consumption, aiming to create a more robust model with limited real-world measurements. The network was trained with data synthesized using, among others, electricity, temperature, and humidity, encoded into receiver operating characteristic (ROC) plots which visually encode the separation between classes and are commonly used to assess model discrimination (Zweig and Campbell, 1993; Janssens and Martens, 2020).

Other researchers focus on creating and applying digital twins: virtual, dynamic, and data-driven digital replicas of real-world urban environments. Stinner et al. (2021) generate digital twins of building energy systems from piping and instrumentation diagrams using convolutional networks and other algorithms. Agostinelli et al. (2021) create digital twins of energy efficient buildings in residential areas from Building Information Modeling (BIM), Internet of Things (IoT), Geographical Information Systems (GIS), and AI components, with machine learning serving as the central module of the model. Francisco et al. (2020) take a different approach by generating digital twins of daily, time-segmented energy benchmarks solely from smart meter data streams. Belik and Rubanenko (2023) present a hybrid digital twin framework for renewable energy sources (RES) that integrates real-time data, 3D modeling, and sensitivity analysis to improve forecasting and operational efficiency, particularly in grid systems with high RES penetration.

While prior work has focused on traditional simulation tools or sensor data to construct digital twins, Xu et al. (2024) encourage the use of generative AI models, such members of the GPT family, because they present new opportunities in urban data generation. For instance, Dodge et al. (2017) employ convolutional neural networks (CNNs) to parse floor plan images, generating structured representations using wall segmentation, object recognition, and optical character recognition. Relatedly, Zhang et al. (2025a) implement a pipeline that generates EnergyPlus IDF files from initial building geometry and textual building descriptions. Moreover, Xiao and Xu (2024) propose

a multi-agent Large Language Model (LLM) framework that processes unstructured building data and sensor logs to support automated energy optimization in smart grid contexts. Additionally, in closely related fields, generative AI has been successfully employed to perform a variety of tasks, such as predictive analysis of traffic congestion (Lin et al., 2025), real-time decision-making in urban air mobility (Sha et al., 2024), and stochastic solar irradiance forecasting for building facades (Zhang et al., 2022).

Liu et al. (2025) present a wide-ranging review on the integration of generative AI into building energy workflows, highlighting both opportunities and challenges. These include concerns such as dataset preparation, hallucinations, and a lack of domain-specific expertise. However, the impact of such challenges varies depending on the pipeline design. Because our framework combines pretrained LLMs with simulation tools for quantitative evaluation, we avoid the need for fine-tuning or physics-aware generation, thereby reducing the impact of these concerns. We evaluate our framework’s LLM components to reduce hallucinations. Additionally, Liu emphasizes the importance of multimodal integration—where multiple data modalities (such as image, text, and tabular data) are used by a process or model. Producing high-quality structured urban data suitable for tasks such as modeling and simulation requires combining multiple complementary processes into a single workflow (Rehmann et al., 2025; Guo et al., 2023; Bishop et al., 2024). We adopt these principles in the design of our general framework.

3 Methodology

We propose a novel framework that combines multimodal real-world data with data generated using LLMs. We leverage open-access county data and generative AI to construct synthetic homes that mirror real-world counterparts and inspection notes corresponding to each. Home inspection notes will be used as a source to rate the homes based on their energy efficiency, alongside home images, floorplans, and simulation results. Finally, we test the LLM components of our framework and the realism of the generated data. Our framework comprises four modular components, depicted in Figure 1, where each stage focuses on a transformation of the data, from data collection to simulation:

1. A web scraper that collects data and images;
2. An image processor powered by LLaVA (Liu et al., 2023);
3. A Geographic JSON (GeoJSON) and inspection note generator using GPT (OpenAI, 2025);
and
4. An EnergyPlus (Crawley et al., 2001) simulation

While our pipeline is tailored to generate data from images and tabular data, it is inherently modular and extensible. Any stage is easily modified or expanded for other related purposes, and different information can be generated in addition to or in place of any data produced by this pipeline. For example, a different LLM could be employed in place of GPT, or other types of data could be considered or generated by the pipeline. Those interested in generating synthetic commercial buildings could use a modified version of this pipeline that emphasizes the characteristics and data central to their research. This opens use of our work to a larger set of individuals. Rather than proposing a rigid set of steps, we present a flexible framework that integrates generative AI, web scraping, and building simulation, designed for rapid, low-cost data generation in building energy



Figure 2: An example street view photograph and floor plan from the county database.

and other fields that traditionally suffer from data scarcity. Ultimately, the data generated by our framework can be used to prototype, design, train, and research urban energy systems and models.

An instance of this pipeline was implemented and executed¹ on a `g3.medium` flavor JetStream 2 virtual machine running Ubuntu 24.04.2 (Noble). Specifically, the system featured one NUMA node with 8 AMD EPYC-Milan processors, 30 GB of RAM, and an NVIDIA A100 SXM4 40 GB GPU (of which 10 GB was allocated). Additionally, it was fully virtualized (KVM and AMD-V). We paid \$0.36 (USD) for OpenAI requests to produce data for 258 homes—about \$0.0014 per home.² To run the pipeline, we used the PyTorch (Ansel et al., 2024) machine learning framework, and the Hugging Face Transformers library (Wolf et al., 2020) to load the models we used. In the subsections that follow, we describe each pipeline component in detail.

3.1 Scraping the Data

To ensure the synthetic data we generated reflects real-world homes, we collected data from publicly available county datasets. For our pipeline instance, we gathered data from [location withheld for double-blind review]. To collect this data, we implemented a web scraper using `Selenium WebDriver` (Selenium, 2024) and `ChromeDriver` (Google, 2023). For each residential property on each street in the list of streets to process, the scraper extracts key attributes, such as number of rooms, total floor area, and other metadata listed in Table 1. This data is saved to a JavaScript Object Notation (JSON) file for each home. Additionally, the scraper downloads two images: a street view photograph and a floor plan, both of which are made available on the county’s public-facing platform. An example of each is depicted in Figure 2.

3.2 Processing Images

After scraping the street view photographs and floor plans from the county portal, they are analyzed using LLaVA (Liu et al., 2023). This step processes both files to translate them into a textual description. For example, the floor plans can be used to define the geometry of the home, and the image to determine the quality and number of windows. The use of images allows our pipeline to

¹Our source code is available at: <https://github.com/Lafayette-EshbaughSilveyra-Group/synthetic-homes>.

²Assuming a conservative upper bound of 10 CPU minutes per home at 100 watts and electricity prices at \$0.15 per kilowatt-hour, local electricity costs are approximately \$0.0025 per synthetic home, giving a worst case total of \$0.0039 per synthetic home.

Collected Data	Type
Year Built	Year
Remodeled Year	Year
Land Use Code	String
Total Square Feet Living Area	Number
Number of Stories	Number
Grade	String
CDU	String
Building Style	String
Total Rooms	Number
Bedrooms	Number
Full Baths	Number
Half Baths	Number
Additional Fixtures	Number
Total Fixtures	Number
Heat/Air Cond	String
Heating Fuel Type	String
Heating System Type	String
Attic Code	String
Unfinished Area	Number
Rec Room Area	Number
Finished Basement Area	Number
Fireplace Openings	Number
Fireplace Stacks	Number
Prefab Fireplaces	Number
Basement Garage (Number of Cars)	Number
Condo Level	Number
Condo/Townhouse Type	String
Basement	String
Exterior Wall Material	String
Physical Condition	String
Sketch Data	Dictionary of floorplan segment areas

Table 1: All data we collected from the county portal. Not all homes have values for each variable.

infer important aspects of the homes that will be used to generate the GeoJSON, which is ultimately used to generate the Input Definition File (IDF) file required by EnergyPlus.

3.2.1 Evaluating Visual Focus with Occlusion Testing

In image processing, it is crucial that only key portions of the images in question trigger differences in the response of a model. We refer to this as *focus*. For example, if the prompt asks about the state of the roof of a home, the tree next to the home should be inconsequential in comparison to the roof itself. To evaluate this, we use a technique called occlusion.

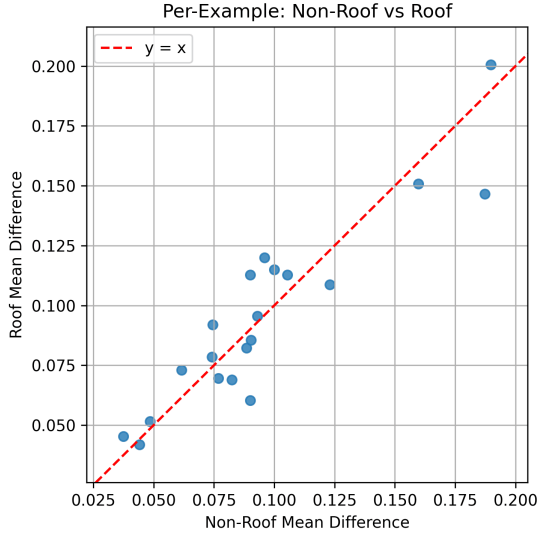
Occlusion measures the necessity of a part of an image: if removing a feature causes the prediction to change, that feature was necessary for the model’s decision (Hooker et al., 2019; Balkir et al., 2022). When we remove image portions, we replace them with a neutral value, such as black. This creates a masked version of the image. The degree of change measured between the model’s output for this masked image and its baseline response reflects the importance of the masked cell. High sensitivity to the removal of a feature suggests the model relied heavily on that region to produce its output, indicating that the region was internally necessary to the model’s decision process.

During the development of our pipeline, we identified two candidate LLMs to employ for image processing. To determine the best model for this task, we compared the focus of the GPT and LLaVA LLMs when analyzing images using occlusion tests. We provided the models with twenty different images of homes: ten with roofs showing no signs of damage, and ten with roofs with significant damage. Each model was instructed to evaluate and describe the state of the roof and justify its evaluation. We first took a baseline where no part of the image was masked. Then, the image was divided into one hundred cells, a number we selected to balance effectiveness, efficiency, and cost. Each cell of the image was masked, and the model was executed on the original prompt and this new image. Textual responses were embedded into vectors using the `all-MiniLM-L6-v2` SentenceTransformers model (Reimers and Gurevych, 2019), a lightweight and widely used model sufficient for obtaining sentence-level numerical representations. Then, to measure the semantic difference between each execution of the experiment, we took the cosine distance of each embedded response from the baseline. Additionally, heatmaps of these differences were assembled using `matplotlib` (The Matplotlib Development Team, 2025).

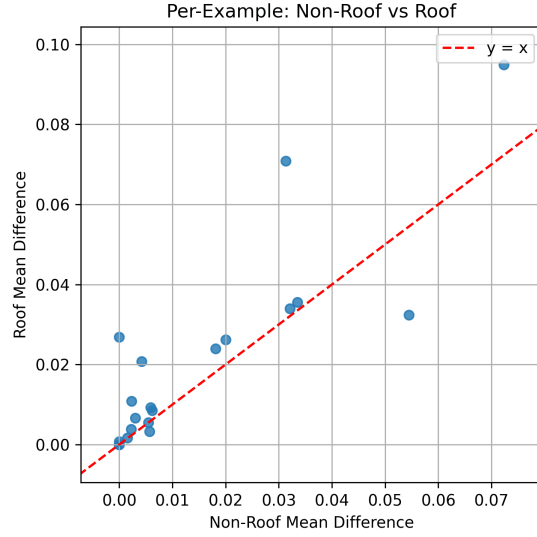
The mean difference value in roof cells and non-roof cells for each image was calculated. Figure 3 depicts the distribution of the forward occlusion results. These scatter plots are particularly telling—GPT (Figure 3a) evenly scatters the data points on either side of the line $y = x$, indicating it has no preference for which area in the image is considered important. In comparison, LLaVA (Figure 3b) tends to produce results in the upper half of the graph. This illustrates LLaVA’s improvement over GPT plainly: more often than not, LLaVA’s response depends more on the roof than other parts of the image.

Additionally, overall means and standard deviations were calculated for GPT and LLaVA (Figure 4). In a well-focused model, the mean difference in the relevant area should be greater than the mean difference anywhere else. This behavior occurs since relevant cells should account for the majority of the response given by the model. In our experiments, we observe that GPT reports identical roof and non-roof mean differences (Figure 4a). However, LLaVA achieved a roof mean difference approximately 20% greater than its non-roof mean difference (Figure 4b).

When we compared individual GPT and LLaVA occlusion results, we found more evidence that LLaVA performs better at focusing on key parts of the images. LLaVA is much more particular about which cells are key to construct the response; GPT produces results that look stochastic. Figure 5 displays one noteworthy example—LLaVA focuses on a more specific section of the image, primarily consisting of the home’s roof. GPT, on the other hand, behaves much more randomly.



(a) GPT results.



(b) LLaVA results.

Figure 3: GPT and LLaVA forward occlusion per image results.

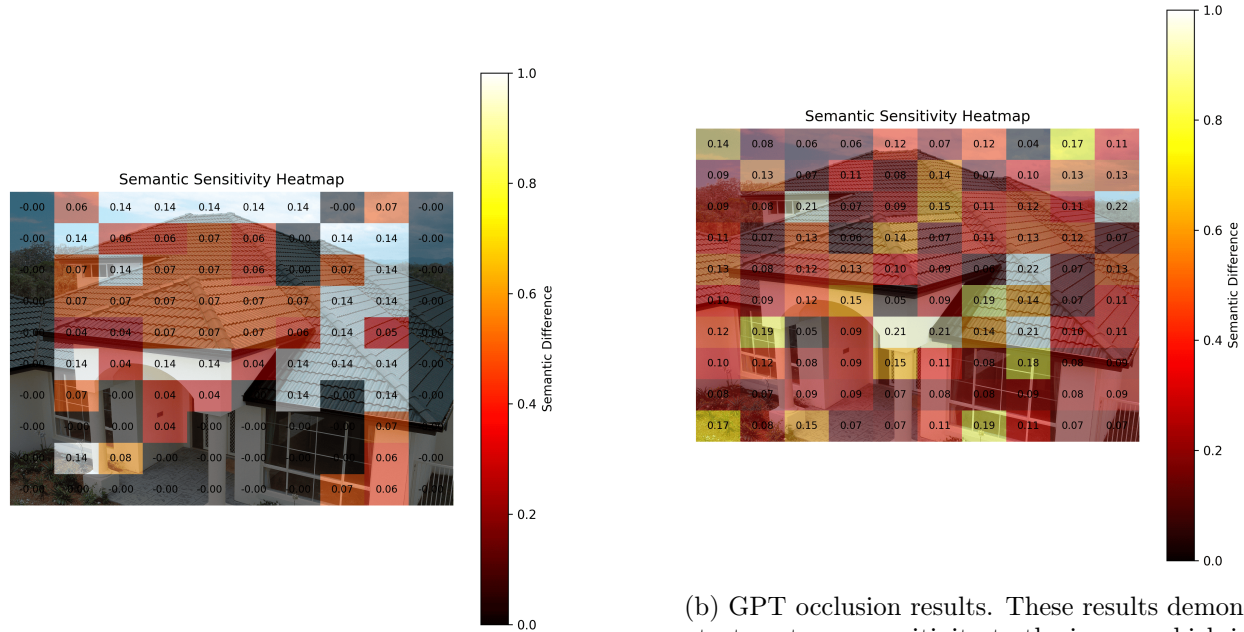
	Mean Difference	SD
Roof	0.0956	0.0384
Non-Roof	0.0956	0.0408

(a) GPT occlusion overall statistics

	Mean Difference	SD
Roof	0.0208	0.0241
Non-Roof	0.0149	0.0197

(b) LLaVA occlusion overall statistics

Figure 4: Occlusion statistics for GPT and LLaVA.



(a) LLaVA occlusion results. These results show less sensitivity and more focus on the more important parts of the image.

(b) GPT occlusion results. These results demonstrate extreme sensitivity to the image, which is not desired. This sensitivity means the model focuses less on the most important parts of the image while responding to the prompt.

Figure 5: GPT and LLaVA occlusion results.

Each value in the cell is the semantic difference, and the background tint of the cell represents the scaled semantic difference, where the brightest background represents the largest difference and the darkest represents the smallest. In Figure 5a, the semantic difference is generally larger on the roof than on other parts of the image. A small semantic difference is a signal that a given portion of the image is less important to the model in order to formulate a response. In Figure 5b, the majority of cells are moderately important to the model in formulating a response—even cells containing walls or grass. Comparing the two, LLaVA demonstrates better focus on the more important parts of the image. Full occlusion experimental details, hypotheses, and findings are available in A.

3.3 Generating GeoJSON

Once the images are processed, we utilize the descriptions given by LLaVA in a GPT prompt (see Appendix B) to generate a GeoJSON file and home inspection notes. The prompt provides the image descriptions (Section 3.2) and data that was scraped from the county portal (Section 3.1) and directs the model to take two actions:

- The prompt instructs GPT to generate a GeoJSON file for the building, including geometry, data from the county, and five estimated performance parameters. These estimated parameters, defined according to standard convention, include the HVAC heating and cooling coefficients of performance, r-values for the roof and wall, and the air change rate.
- The prompt directs GPT to write a short inspection note, focused on energy-related observations such as insulation, HVAC type/age, visible windows, and any inferred upgrades. This inspection note is placed in the GeoJSON file.

```

1 {
2   "type": "Feature",
3   "properties": {
4     "name": "Generated Home",
5     "floor_area": 2576,
6     "building_type": "Single family",
7     "inspection_note": "...",
8     "hvac_heating_cop": 0.85,
9     "hvac_cooling_cop": 3.0,
10    "wall_r_value": 13,
11    "roof_r_value": 30,
12    "air_change_rate": 0.35
13  },
14  "geometry": {
15    "type": "Polygon",
16    "coordinates": [...]
17  }
18 }

```

Figure 6: Excerpt of a generated GeoJSON file.

The prompt contains strict guidelines to ensure outputs are valid, accurate, and complete. An excerpt from an example GeoJSON object is provided in Figure 6.

We use GPT for structured data generation given its strong ability to produce well-formed JSON outputs from descriptive prompts. Multiple studies have shown that LLMs perform well on generation tasks under strict schema constraints, even with no previous prompting or fine tuning. For example, StructuredRAG’s benchmark suite showed 82% format compliance under JSON prompt conditions (Shorten et al., 2024). As we built the pipeline, we reviewed GPT’s responses and it seldom failed to adhere to the JSON structure. In the rare case that it doesn’t, our program catches the JSON error and automatically reprompts GPT for that example.

3.4 Running EnergyPlus Simulations

To execute a simulation in EnergyPlus, we take the GeoJSON generated by GPT (Section 3.3) and convert it to an IDF file for use in EnergyPlus. We use a template IDF file, filled with default values that are replaced with variables from the GeoJSON data, such as the geometry, HVAC heating and cooling coefficients of performance, r-values for the wall and roof, and the air change rate. Additionally, the template has many fields with constant values, such as the simulation running period and materials, constructions, and zones used in the simulation. Once the details from the GeoJSON are copied into the template, a final IDF file is produced.

The templating process is facilitated with the `eppy` package (santoshphilip, 2024), which makes programmatic IDF generation straightforward. Then, we use `ExpandObjects` to prepare the file for simulation. `ExpandObjects` is bundled with EnergyPlus, and its primary use case is to take an IDF and expand template objects—such as the `HVACTemplate` we use—into full systems (U.S. Department of Energy, 2023). Finally, we run the expanded IDF file through EnergyPlus, producing final simulation results.

We write the inspection notes and EnergyPlus simulation results for each example into one JSON Lines (JSONL) file. This completes our end-to-end dataset generation process, yielding a unified dataset that combines textual and simulation-based information.

Variable	Overlap (%)	ResStock IQR (Q1–Q3)	Synthetic Mean	Synthetic Median
Wall R-Value	93.41	0.704 (1.94–2.64)	2.79	2.29
Roof R-Value	100.0	3.35 (3.35–6.69)	5.04	5.28
Cooling COP	66.28	0.70 (3.1–3.8)	2.99	3.00
Heating COP	100.0	0.20 (0.8–1.0)	0.84	0.85

Table 2: Coverage of synthetic homes within the 10–90% ResStock range, alongside ResStock interquartile ranges (Q1–Q3) and synthetic homes mean and median.

4 Validating Realism of Pipeline Generated Data

Following prior work on synthetic data evaluation (Goncalves et al., 2020; Patki et al., 2016), we adopt the definition of realism as the overlap of synthetic values with the 10%–90% range of a trusted reference on the home characteristics being generated. To measure the realism of our generated data, we compare it with ResStock (Present et al., 2024; Reyna et al., 2025), a dataset that contains realistic samples of homes in different regions of the United States as IDF files. The analysis consists of performing statistical analyses comparing the distribution of values in our synthetic homes to those in ResStock. We only use ResStock data from climate zone 4A, the region in which the synthetic homes are collected in our example, and we only compare the four pre-selected variables—Wall R-Value, Roof R-Value, Cooling Coefficient of Performance (COP), Heating COP—that are not static among all synthetic homes. The number of synthetic homes is 258 while the number of climate zone 4A ResStock samples is 2000.

Table 2 reports the realism for the four variables across all synthetic homes by displaying the percentage of values that overlap with the 10%–90% range of ResStock. We found overlap greater than 65% for all variables and greater than 90% for three variables. This overlap is a strong indicator of realism for our generated data. Additionally, the table includes the mean and median of the four variables for all synthetic homes and the interquartile range (IQR) of the four variables for all ResStock homes. These statistics are included for informational purposes and are not considered when determining realism.

The results above and the tests of the generative components of our framework demonstrate a level of confidence above previous work such as Zhang et al. (2025a) and Xiao and Xu (2024). These works and others either accept the output of the LLMs or use procedural evaluation techniques.

Occlusion offers stronger empirical support that the image processing component of our pipeline—which is LLM-based—performs as expected. We additionally demonstrated statistically that properties of our generated homes are realistically distributed according to ResStock. Our results directly address and mitigate concerns about hallucination and unreliability raised in prior work (Liu et al., 2025). It is fair to be skeptical of LLMs and other ML models—but with our results, we clearly demonstrate our pipeline is not as susceptible to some of the issues Liu et al. (2025) raise.

5 Conclusion

In this work, we presented a novel way to generate multimodal building-scale data for urban energy research and other related fields. Using a multimodal pipeline, we produced this data in a cost-effective and efficient way. We also performed an in-depth analysis to ensure that our generative AI pipeline components were behaving as expected, taking into account the concerns of Liu et al. (2025).

Generative AI is a powerful tool, and we recognize the importance of this new frontier as described

by Xu et al. (2024) and Liu et al. (2025). Not only does our work demonstrate a step forward in the urban energy field, it also presents a useful, malleable tool that experts and researchers can use for a variety of tasks.

One promising direction is the use of this pipeline to train ML algorithms. A natural expansion of the pipeline could utilize the resulting EnergyPlus simulation data and inspection notes to rank the efficiency of particular components that affect the energy efficiency of a home. These labeled homes could be used as inputs for an ML model that could provide recommendations for energy efficiency retrofits. Furthermore, this model, trained with our synthetic data, could be used to predict the priorities for retrofits in real houses.

Overall, the high prices, lack of availability, or privacy concerns attached to the collection of urban energy data can be avoided by generating synthetic data. With our framework, all of these concerns are alleviated and realistic data is produced. This reduced dependence on costly or restricted data sources provides a pathway towards more accessible research.

A Occlusion Results

In this appendix, we provide detailed information and results from our occlusion tests. Firstly, when running the test we utilized identical prompts for each model. For GPT, we prompted:

You are a certified home inspector. Describe the status roof. Is it in good condition?
Why or why not?

Likewise, we prompted LLaVA with the following:

USER: <image>
You are a certified home inspector. Describe the status roof. Is it in good condition?
Why or why not? ASSISTANT:

These prompts differ slightly due to how the models are trained; namely, LLaVA expects an image token and labeled portions of the message. The majority of LLMs behave this way, and the GPT API likely wraps the given prompt in something similar.

Next, we provide our hypotheses pertaining to the performance of both models. We hypothesize that LLaVA’s advantage stems from its architecture: it employs an early fusion design in which images are converted into visual tokens by CLIP (Radford et al., 2021) that are then prepended to the textual prompt (Liu et al., 2023). These visual tokens are passed through the transformer layers of the LLM together with text tokens, enabling multimodal attention at every layer. It has been demonstrated that vision tokens are most critical for a model in early layers, when they fuse into text tokens (Zhang et al., 2025b). A likely result of this is the reduction of the model’s sensitivity to variations in the image, which may explain its stronger performance in our experiments.

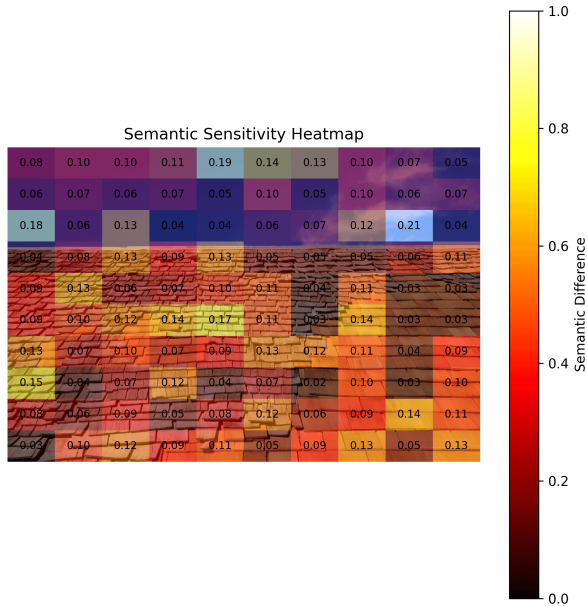
While GPT-4V (GPT’s vision model) is proprietary, the case can be made that it possesses a different structure. Evaluation studies show that it performs well across visual reasoning and captioning tasks, but it falls short in fine grained visual problems, requiring complex visual tasks to be broken up into interleaved subfigures and text (Yang et al., 2023). These evaluations are similar to evaluations from late fusion (connector) models. For example, BLIP-2 shows strengths in captioning images and instruction-following, while it is less robust with fine-grained spatial reasoning (Li et al., 2023). Another model, MiniGPT-4, demonstrates a similar profile: it has strengths in tasks such as image description, but falters with complex spatial reasoning (Zhu et al., 2023). Both BLIP-2 and MiniGPT-4 are late fusion models, where compressed visual features are routed into the LLM

at later stages (Li et al., 2023; Zhu et al., 2023). As shown, BLIP-2, MiniGPT-4, and GPT-4V all suffer from a very similar weakness: fine-grained or complex spatial reasoning. Based on this similarity, we hypothesize that GPT-4V is also a late fusion model. This helps explain why GPT performed differently from LLaVA in our experiments: as structure dictates function, differences in behavior strongly suggest differences in design. On the basis of this analysis, we feel confident to select LLaVA to complete this task.

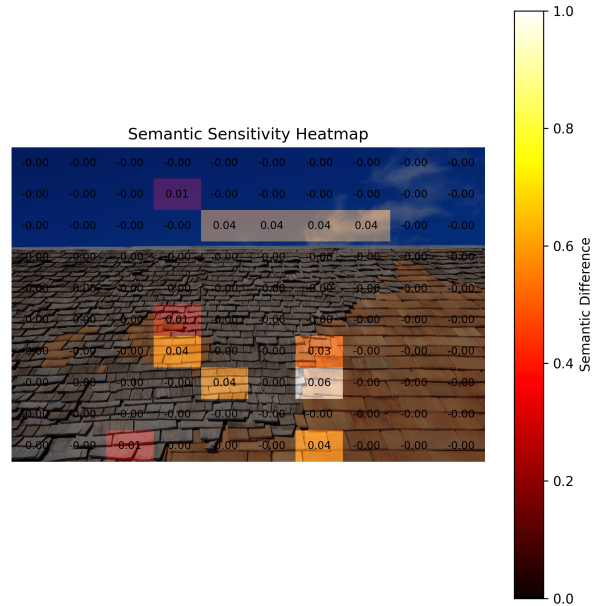
In Table 3, we provide our forward occlusion results, including roof mean difference (RMD) and non-roof mean difference (NRMD) values from both GPT and LLaVA and references to figures displaying GPT and LLaVA heatmaps side by side.

Metric	1	2	3	4	5	6	7	8	9	10
<i>Damaged Roofs</i>										
GPT RMD	0.0856	0.0920	0.0730	0.0689	0.1127	0.0453	0.0516	0.0603	0.1149	0.0419
GPT NRMD	0.0903	0.0745	0.0615	0.0824	0.0900	0.0375	0.0485	0.0900	0.1000	0.0442
LLaVA RMD	0.0033	0.0324	0.0949	0.0093	0.0262	0.0269	0.0356	0.0055	0.0038	0.0208
LLaVA NRMD	0.0057	0.0545	0.0723	0.0059	0.0200	0.0000	0.0335	0.0055	0.0022	0.0042
Roof Cells	70	80	53	83	97	96	80	96	91	88
Non-Roof Cells	30	20	47	17	3	4	20	4	9	12
Figure	7	8	9	10	11	12	13	14	15	16
<i>Undamaged Roofs</i>										
GPT RMD	0.1128	0.0785	0.1465	0.1508	0.0822	0.0956	0.1087	0.2005	0.0696	0.1200
GPT NRMD	0.1055	0.0742	0.1872	0.1598	0.0884	0.0930	0.1230	0.1898	0.0768	0.0959
LLaVA RMD	0.0709	0.0085	0.0007	0.0000	0.0340	0.0108	0.0066	0.0000	0.0017	0.0240
LLaVA NRMD	0.0313	0.0062	0.0000	0.0000	0.0321	0.0023	0.0030	0.0000	0.0015	0.0181
Roof Cells	53	47	68	49	81	39	70	60	47	73
Non-Roof Cells	47	53	32	51	19	61	30	40	53	27
Figure	17	18	19	20	21	22	23	24	25	26

Table 3: Quantitative results from our forward occlusion experiments, including roof mean difference (RMD) and non-roof mean difference (NRMD) for both GPT and LLaVA. The number of cells in the image considered roof and non-roof are listed, and figures of side by side comparisons of the resulting heatmaps are referenced.

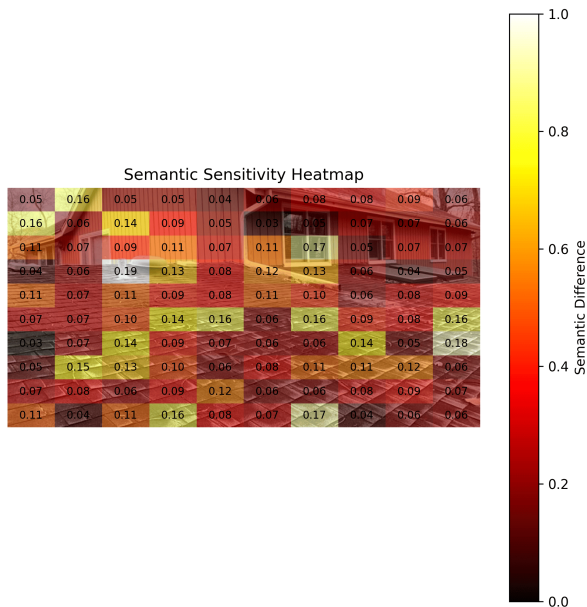


(a) GPT Heatmap

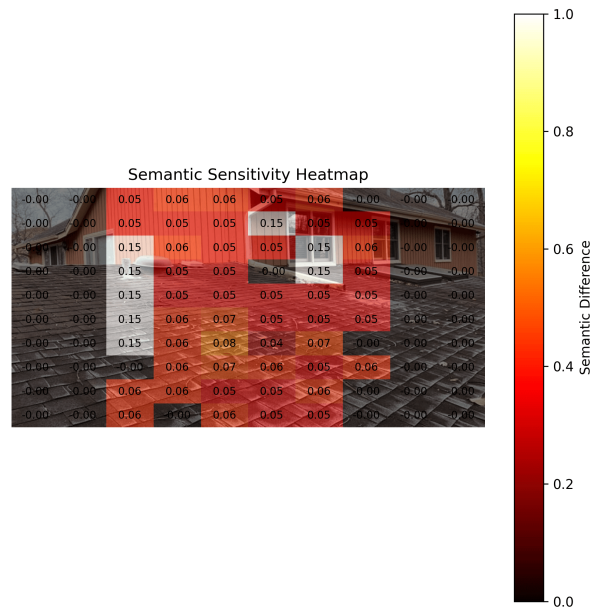


(b) LLaVA Heatmap

Figure 7: Forward Occlusion—Damaged Roof 1

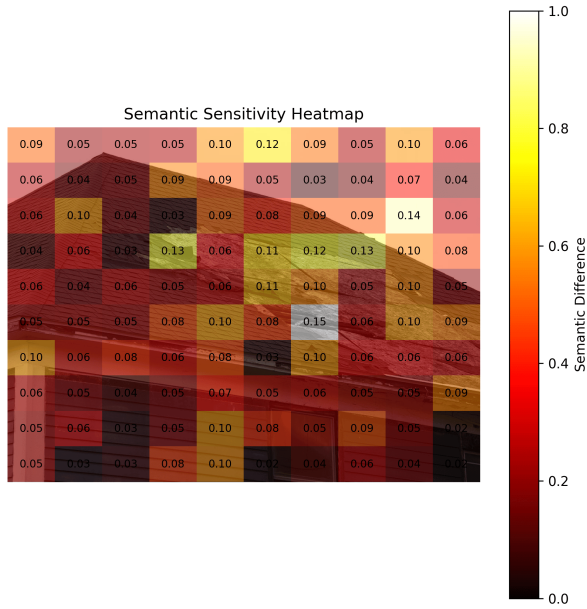


(a) GPT Heatmap

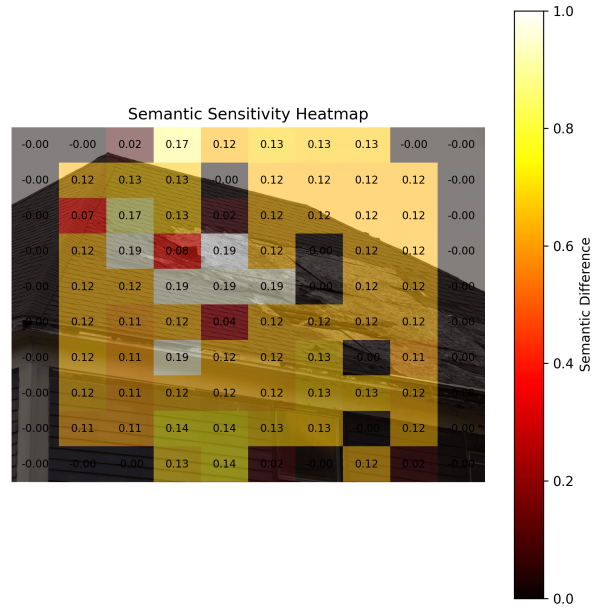


(b) LLaVA Heatmap

Figure 8: Forward Occlusion—Damaged Roof 2

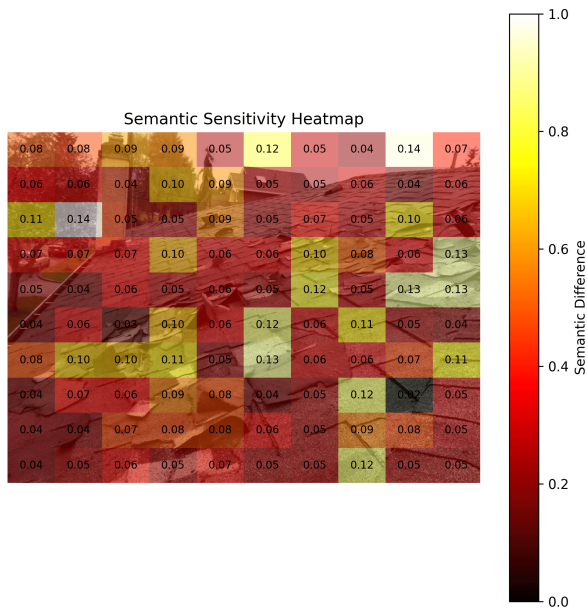


(a) GPT Heatmap

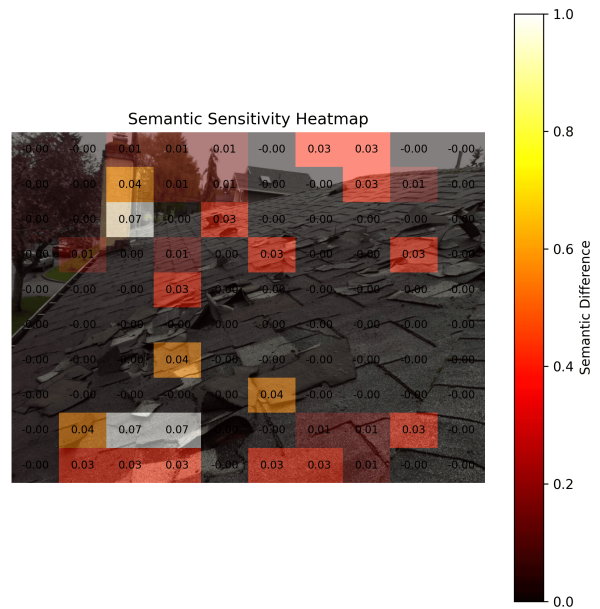


(b) LLaVA Heatmap

Figure 9: Forward Occlusion—Damaged Roof 3

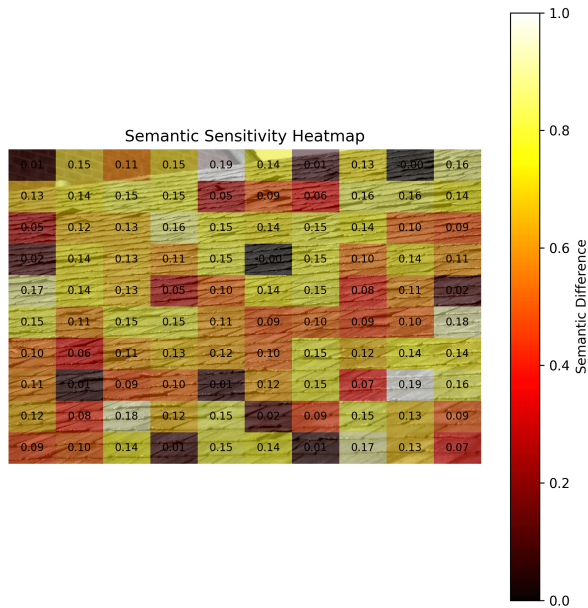


(a) GPT Heatmap

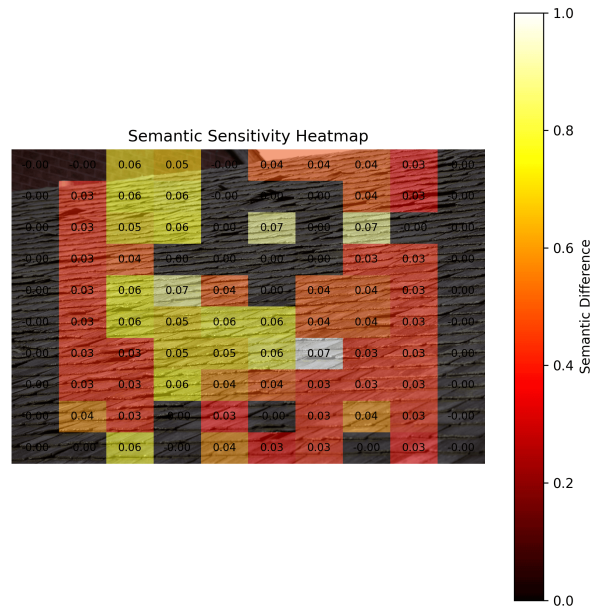


(b) LLaVA Heatmap

Figure 10: Forward Occlusion—Damaged Roof 4

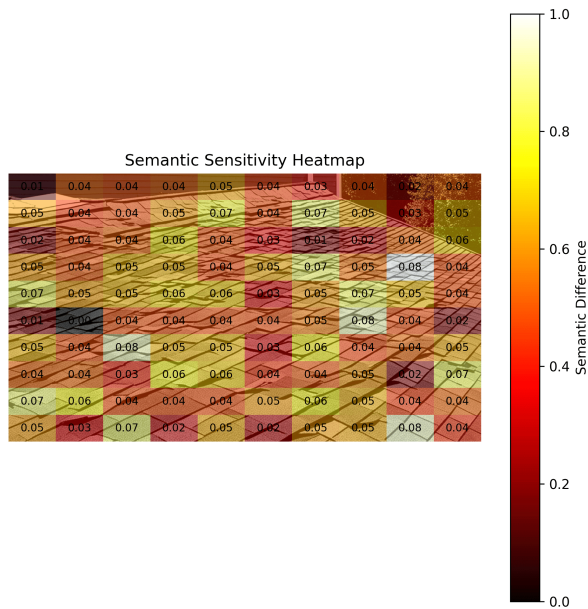


(a) GPT Heatmap

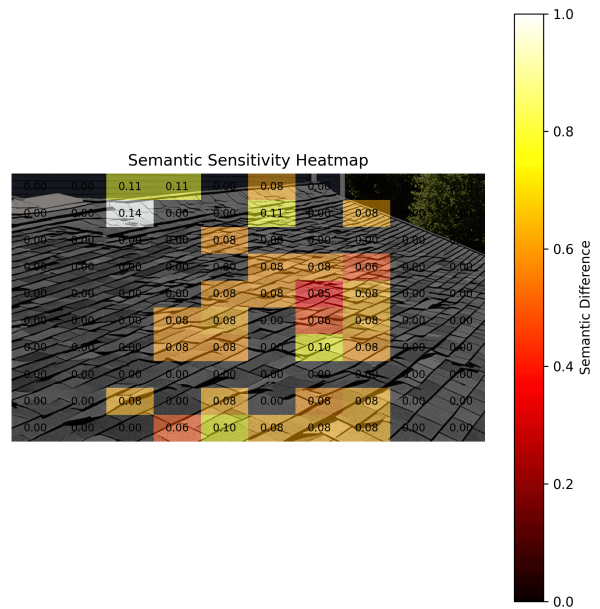


(b) LLaVA Heatmap

Figure 11: Forward Occlusion—Damaged Roof 5

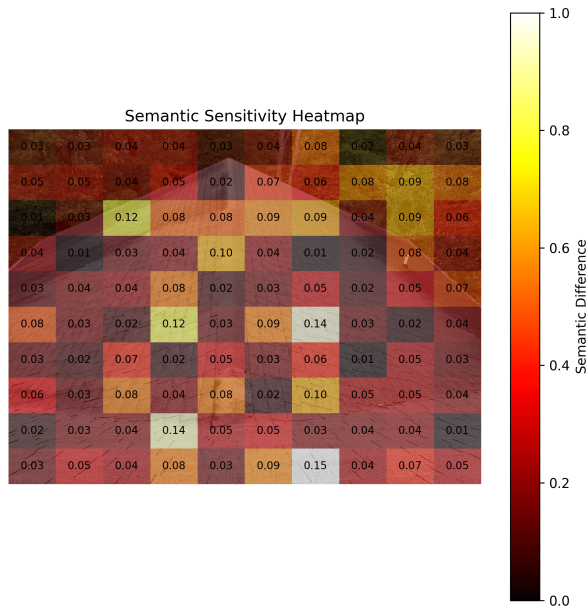


(a) GPT Heatmap

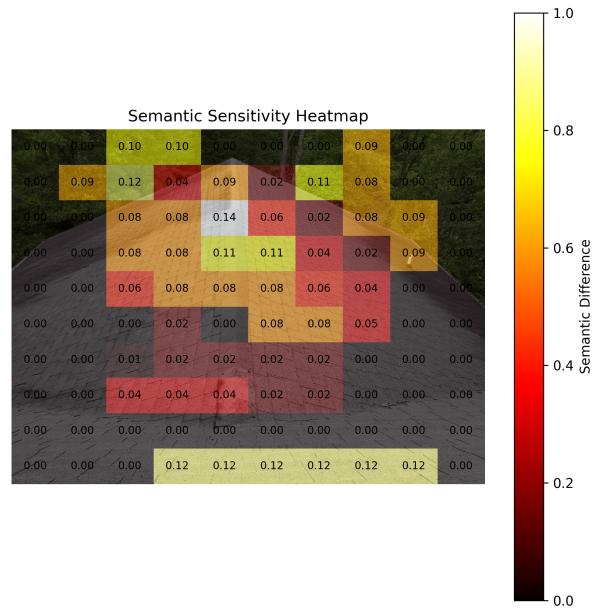


(b) LLaVA Heatmap

Figure 12: Forward Occlusion—Damaged Roof 6

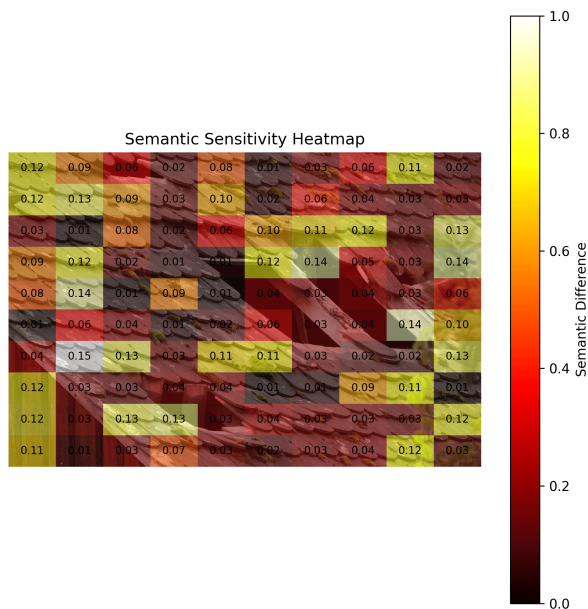


(a) GPT Heatmap

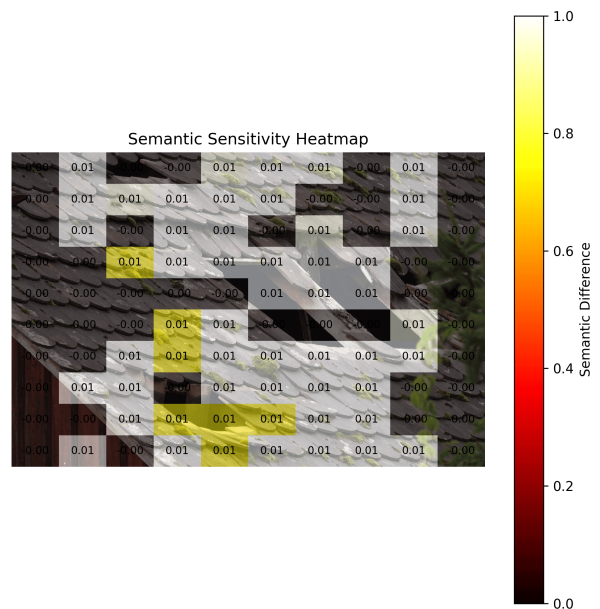


(b) LLaVA Heatmap

Figure 13: Forward Occlusion—Damaged Roof 7

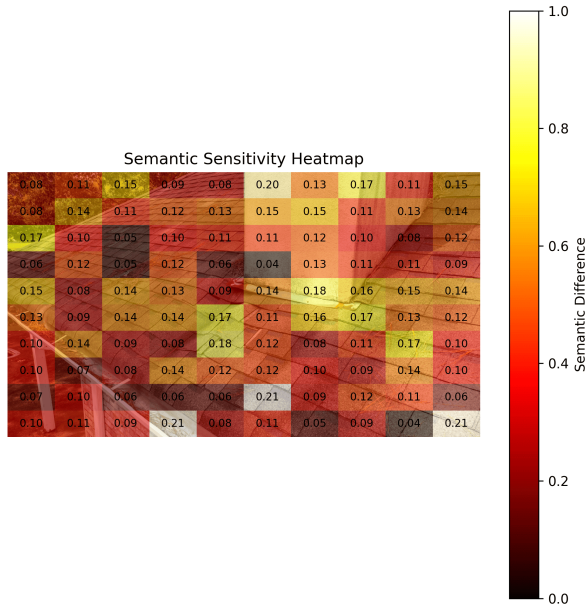


(a) GPT Heatmap

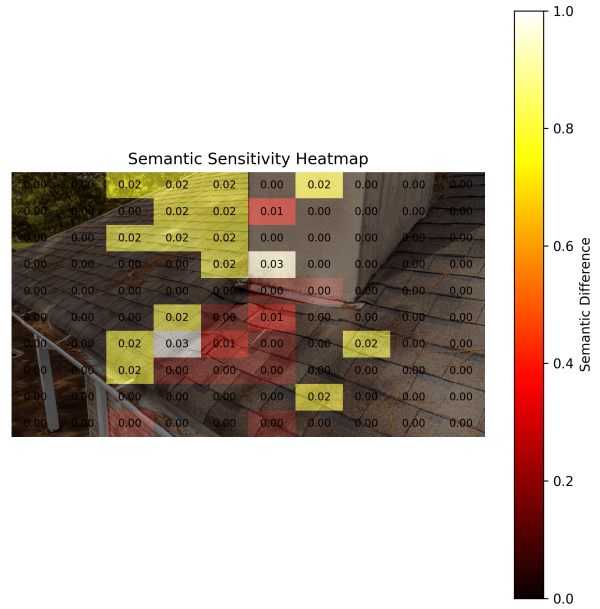


(b) LLaVA Heatmap

Figure 14: Forward Occlusion—Damaged Roof 8

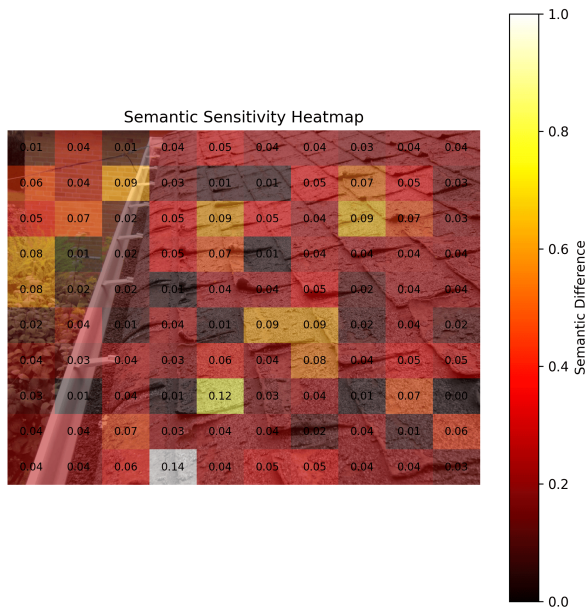


(a) GPT Heatmap

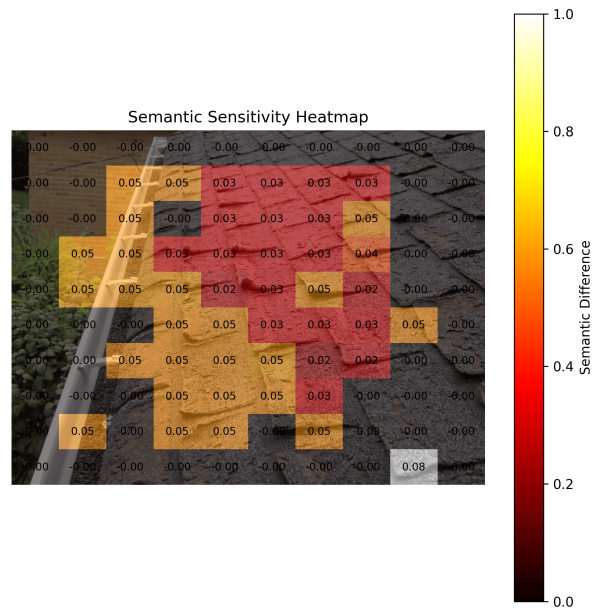


(b) LLaVA Heatmap

Figure 15: Forward Occlusion—Damaged Roof 9

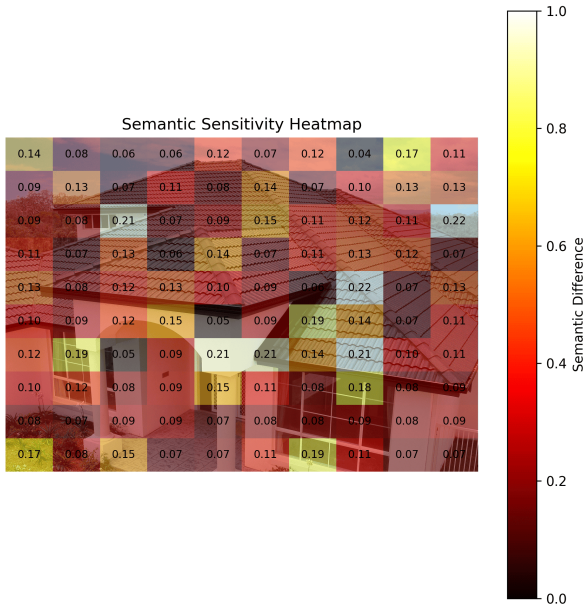


(a) GPT Heatmap

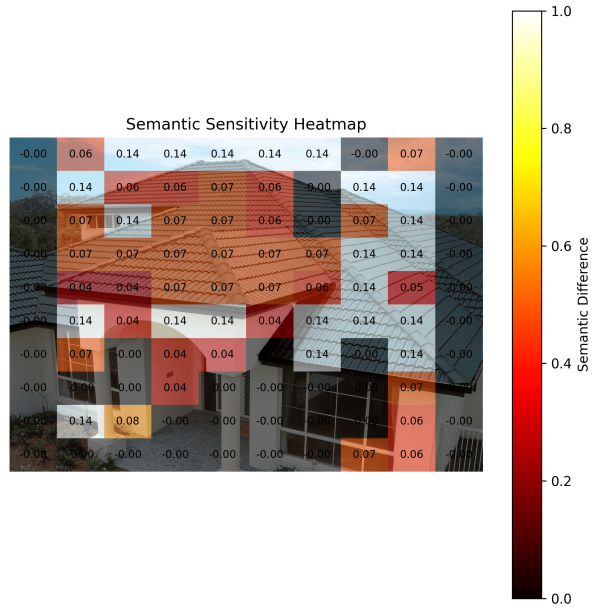


(b) LLaVA Heatmap

Figure 16: Forward Occlusion—Damaged Roof 10

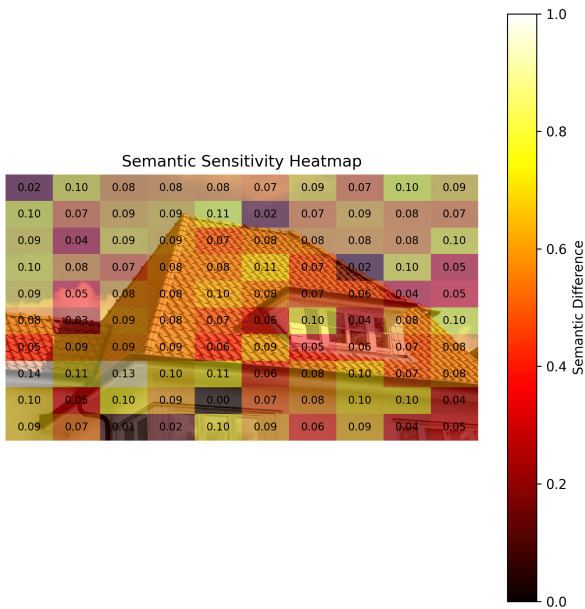


(a) GPT Heatmap

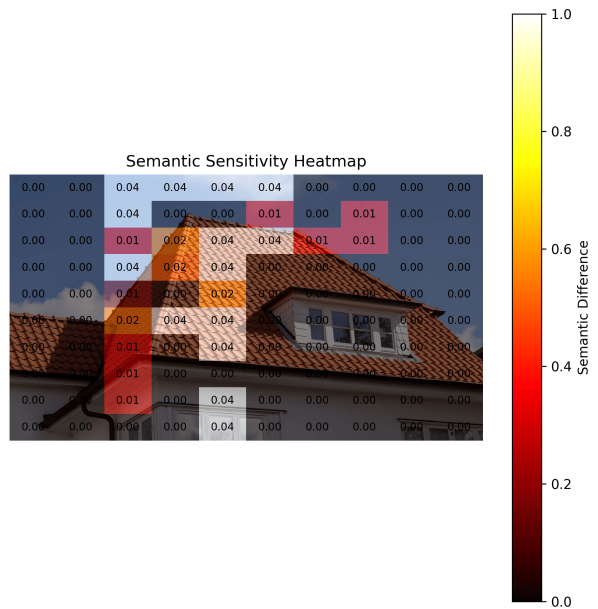


(b) LLaVA Heatmap

Figure 17: Forward Occlusion—Undamaged Roof 1

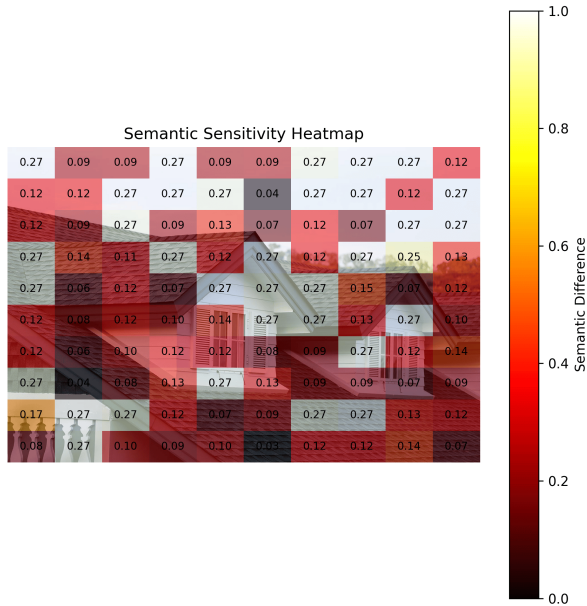


(a) GPT Heatmap

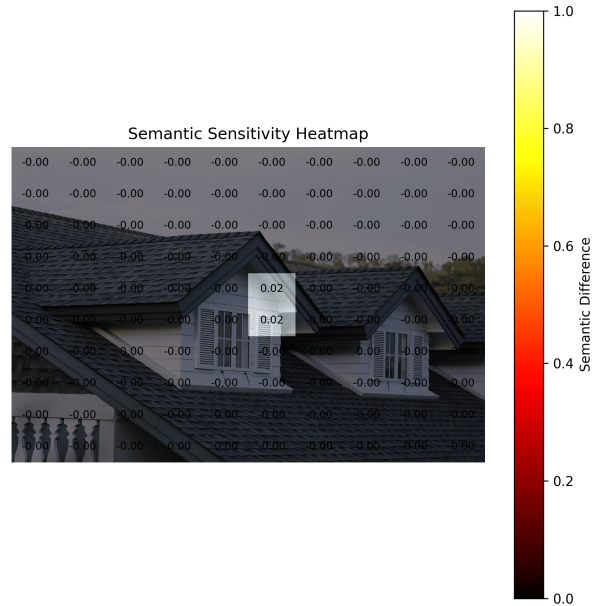


(b) LLaVA Heatmap

Figure 18: Forward Occlusion—Undamaged Roof 2

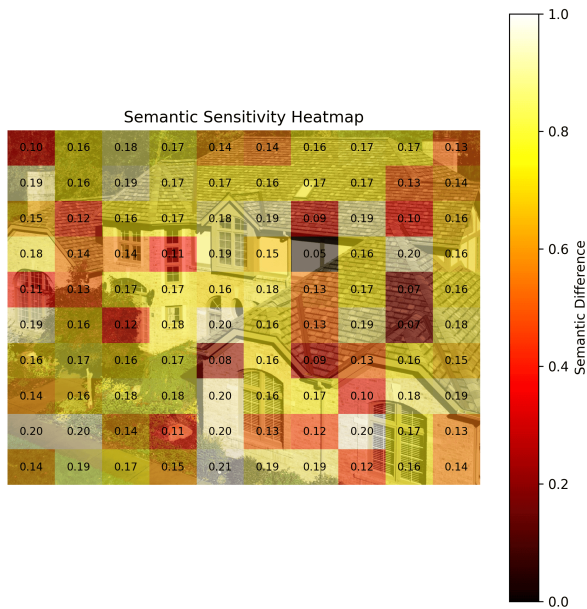


(a) GPT Heatmap

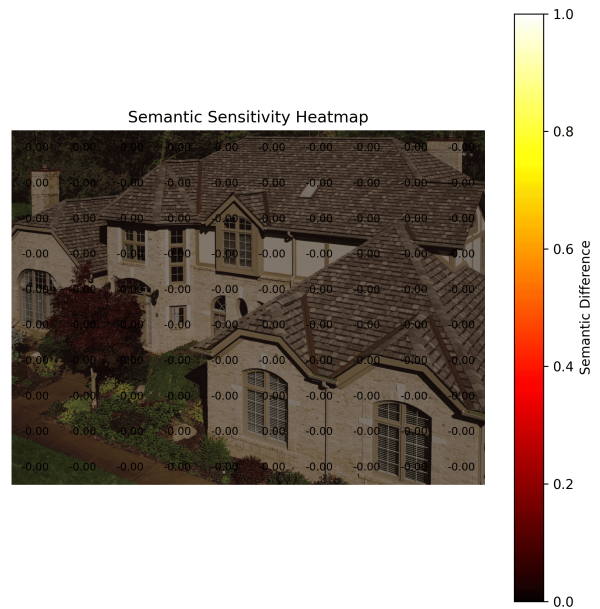


(b) LLaVA Heatmap

Figure 19: Forward Occlusion—Undamaged Roof 3

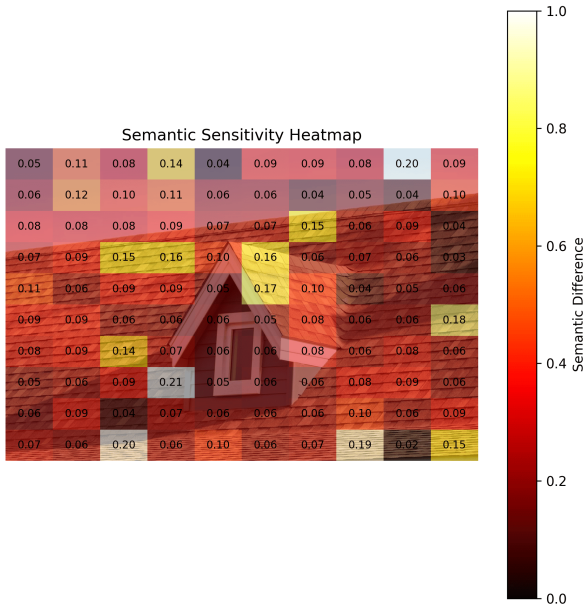


(a) GPT Heatmap

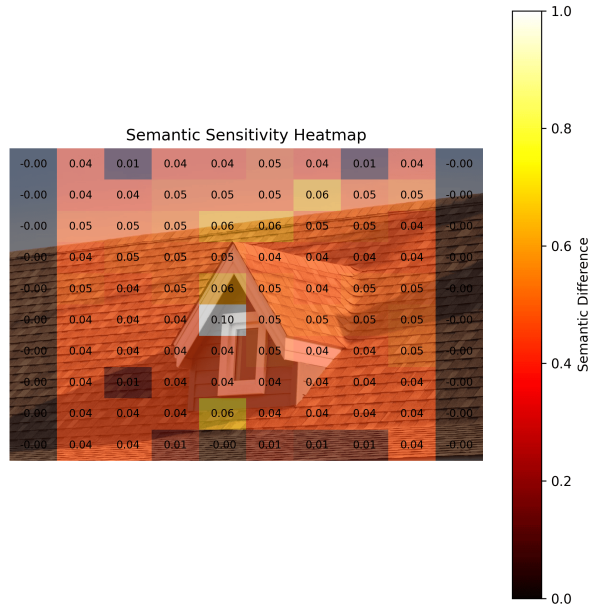


(b) LLaVA Heatmap

Figure 20: Forward Occlusion—Undamaged Roof 4

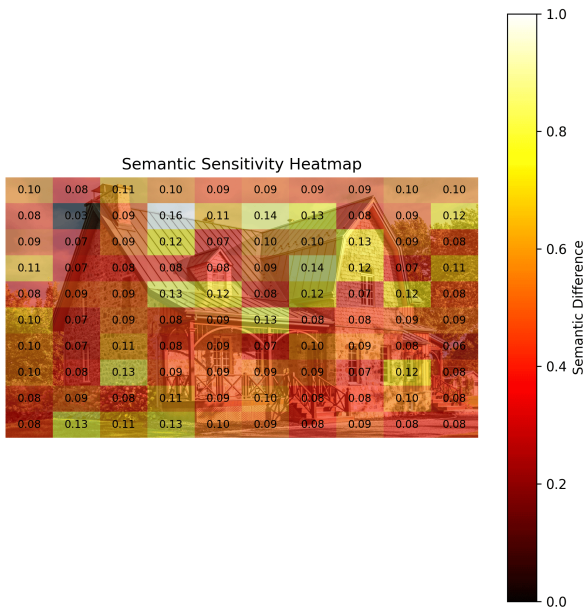


(a) GPT Heatmap

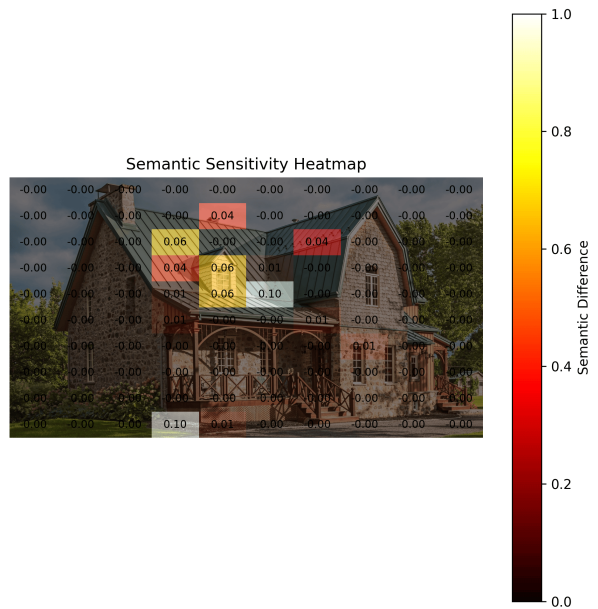


(b) LLaVA Heatmap

Figure 21: Forward Occlusion—Undamaged Roof 5

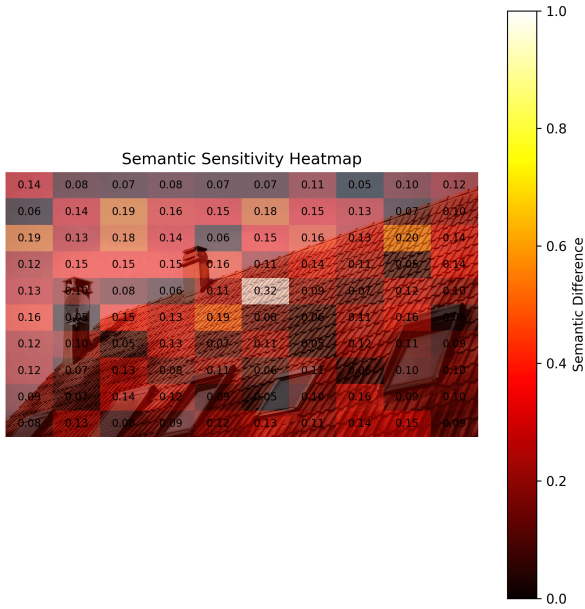


(a) GPT Heatmap

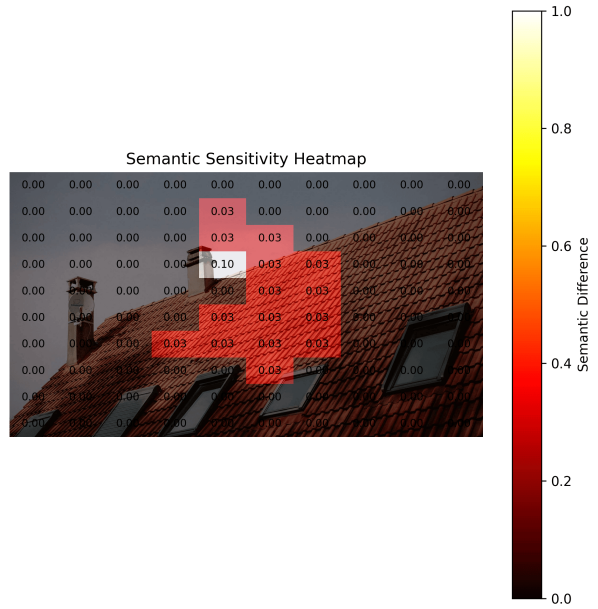


(b) LLaVA Heatmap

Figure 22: Forward Occlusion—Undamaged Roof 6

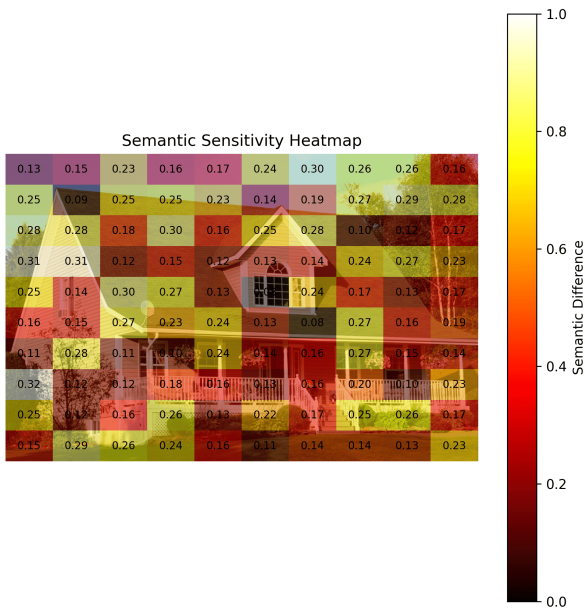


(a) GPT Heatmap

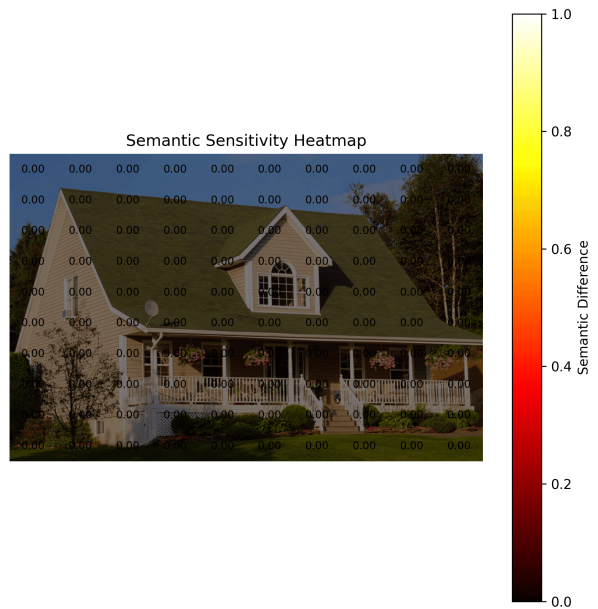


(b) LLaVA Heatmap

Figure 23: Forward Occlusion—Undamaged Roof 7

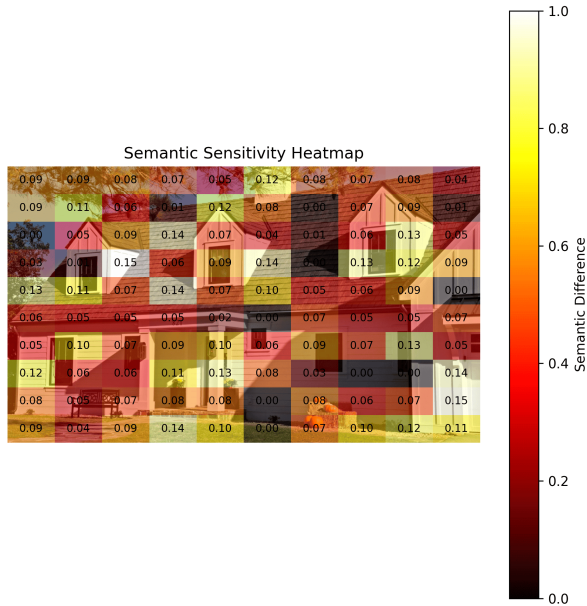


(a) GPT Heatmap

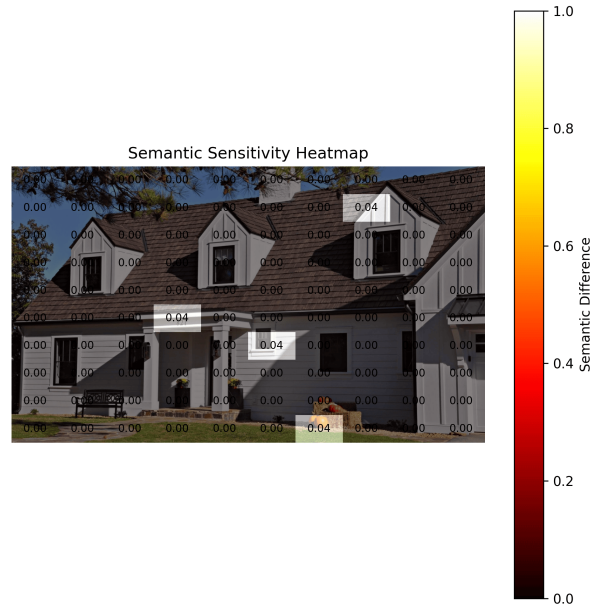


(b) LLaVA Heatmap

Figure 24: Forward Occlusion—Undamaged Roof 8

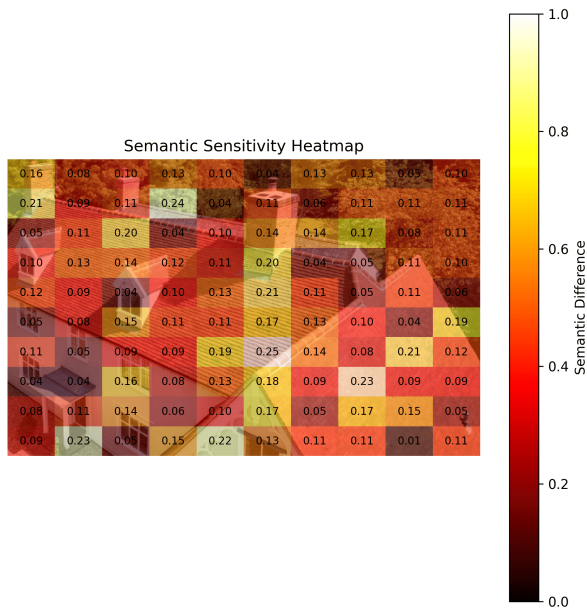


(a) GPT Heatmap

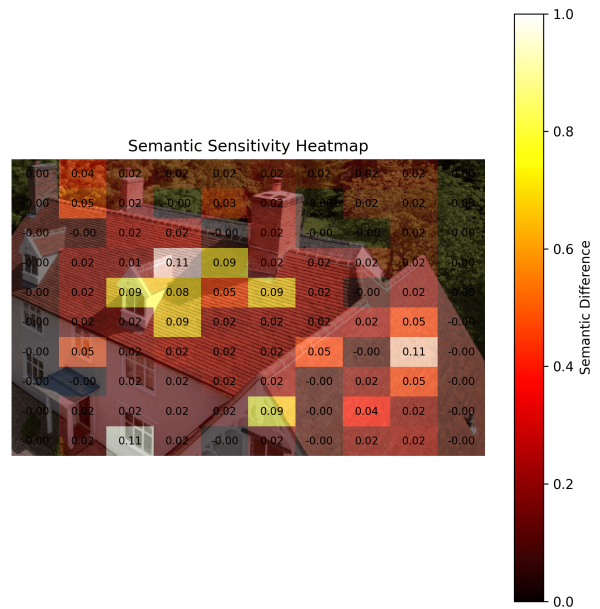


(b) LLaVA Heatmap

Figure 25: Forward Occlusion—Undamaged Roof 9



(a) GPT Heatmap



(b) LLaVA Heatmap

Figure 26: Forward Occlusion—Undamaged Roof 10

B GeoJSON Generation Prompt

In this appendix, we provide the prompt used to generate the GeoJSON data in Section 3.3.

You are a certified home energy inspection expert and data specialist building synthetic training data for an AI model.

You are provided with:

- Structured residential property data (JSON).
- A detailed exterior description of the home: "{exterior_description}"
- A detailed floorplan description: "{floorplan_description}"

Your tasks:

1. Generate a GeoJSON file for this building with:
 - A plausible (longitude, latitude) location in Bethlehem, PA.
 - A FeatureCollection containing exactly one Feature.
 - Geometry: Polygon or MultiPolygon representing the building footprint, realistic for the reported square footage and building style.
 - Properties from the provided JSON:
 - Year Built
 - Total Square Feet Living Area
 - Building Style
 - Exterior Wall Material
 - Heating Fuel Type
 - Heating System Type
 - Heat/Air Cond
 - Bedrooms
 - Full Baths
 - Half Baths
 - Basement
 - Number of Stories
 - Grade
 - Estimated performance parameters:
 - hvac_heating_cop (0--1)
 - hvac_cooling_cop
 - wall_r_value
 - roof_r_value
 - air_change_rate (0--1)
2. Write a short inspection note as if you had toured the home, focusing on energy-related observations.

Strict Guidelines:

- Only base outputs on the provided data and descriptions.
- Do not invent unsupported details.
- Ensure the GeoJSON is valid and realistic.
- Coordinates must plausibly place the home in Bethlehem, PA.

Structured property data:

```
{json.dumps(house_data)}
```

Output format:

```
{  
  "geojson": {
```

```

"type": "FeatureCollection",
"features": [
  {
    "type": "Feature",
    "geometry": { ... },
    "properties": {
      ...,
      "air_change_rate": ...,
      "hvac_heating_cop": ...,
      "hvac_cooling_cop": ...,
      "wall_r_value": ...,
      "roof_r_value": ...
    }
  }
]
},
"inspection_note": "...
}

```

No backticks or explanation.

Glossary

This document is incomplete. The external file associated with the glossary ‘main’ (which should be called `main_preprint.gls`) hasn’t been created.

Check the contents of the file `main_preprint.glo`. If it’s empty, that means you haven’t indexed any of your entries in this glossary (using commands like `\gls` or `\glsadd`) so this list can’t be generated. If the file isn’t empty, the document build process hasn’t been completed.

If you don’t want this glossary, add `nomain` to your package option list when you load `glossaries-extra.sty`. For example:

```
\usepackage[nomain]{glossaries-extra}
```

Try one of the following:

- Add `automake` to your package option list when you load `glossaries-extra.sty`. For example:

```
\usepackage[automake]{glossaries-extra}
```

- Run the external (Lua) application:

```
makeglossaries-lite.lua "main_preprint"
```
- Run the external (Perl) application:

```
makeglossaries "main_preprint"
```

Then rerun \LaTeX on this document.

This message will be removed once the problem has been fixed.

Acronyms

This document is incomplete. The external file associated with the glossary ‘acronym’ (which should be called `main_preprint.acr`) hasn’t been created.

Check the contents of the file `main_preprint.acn`. If it's empty, that means you haven't indexed any of your entries in this glossary (using commands like `\gls` or `\glsadd`) so this list can't be generated. If the file isn't empty, the document build process hasn't been completed.

Try one of the following:

- Add `automake` to your package option list when you load `glossaries-extra.sty`. For example:

```
\usepackage[automake]{glossaries-extra}
```
- Run the external (Lua) application:

```
makeglossaries-lite.lua "main_preprint"
```
- Run the external (Perl) application:

```
makeglossaries "main_preprint"
```

Then rerun \LaTeX on this document.

This message will be removed once the problem has been fixed.

References

- Sofia Agostinelli, Fabrizio Cumo, Giambattista Guidi, and Claudio Tomazzoli. Cyber-Physical Systems Improving Building Energy Management: Digital Twin and Artificial Intelligence. *Energies*, 14(8):2338, April 2021. ISSN 1996-1073. doi: 10.3390/en14082338.
- Jason Ansel, Edward Yang, Horace He, Natalia Gimelshein, Animesh Jain, Michael Voznesensky, Bin Bao, Peter Bell, David Berard, Evgeni Burovski, Geeta Chauhan, Anjali Chourdia, Will Constable, Alban Desmaison, Zachary DeVito, Elias Ellison, Will Feng, Jiong Gong, Michael Gschwind, Brian Hirsh, Sherlock Huang, Kshiteej Kalambarkar, Laurent Kirsch, Michael Lazos, Mario Lezcano, Yanbo Liang, Jason Liang, Yinghai Lu, C. K. Luk, Bert Maher, Yunjie Pan, Christian Puhersch, Matthias Reso, Mark Saroufim, Marcos Yukio Siraichi, Helen Suk, Shunting Zhang, Michael Suo, Phil Tillet, Xu Zhao, Eikan Wang, Keren Zhou, Richard Zou, Xiaodong Wang, Ajit Mathews, William Wen, Gregory Chanan, Peng Wu, and Soumith Chintala. PyTorch 2: Faster Machine Learning Through Dynamic Python Bytecode Transformation and Graph Compilation. In *Proceedings of the 29th ACM International Conference on Architectural Support for Programming Languages and Operating Systems, Volume 2*, pages 929–947, La Jolla CA USA, April 2024. ACM. ISBN 979-8-4007-0385-0. doi: 10.1145/3620665.3640366.
- Esma Balkir, Isar Nejadgholi, Kathleen Fraser, and Svetlana Kiritchenko. Necessity and Sufficiency for Explaining Text Classifiers: A Case Study in Hate Speech Detection. In *Proceedings of the 2022 Conference of the North American Chapter of the Association for Computational Linguistics: Human Language Technologies*, pages 2672–2686, Seattle, United States, 2022. Association for Computational Linguistics. doi: 10.18653/v1/2022.naacl-main.192.
- Milan Belik and Olena Rubanenko. Implementation of Digital Twin for Increasing Efficiency of Renewable Energy Sources. *Energies*, 16(12):4787, June 2023. ISSN 1996-1073. doi: 10.3390/en16124787.
- Daniel Bishop, Patricio Gallardo, and Baxter L. M. Williams. A Review of Multi-Domain Urban Energy Modelling Data. *Clean Energy and Sustainability*, 2(4):10016–10016, 2024. ISSN 2959-7676. doi: 10.70322/ces.2024.10016. URL <https://www.sciepublish.com/article/pii/298>.

- Ettore F. Bompard, Stefania Conti, Marcelo J. Masera, and Gian Giuseppe Soma. A New Electricity Infrastructure for Fostering Urban Sustainability: Challenges and Emerging Trends. *Energies*, 17(22):5573, November 2024. ISSN 1996-1073. doi: 10.3390/en17225573.
- Drury B. Crawley, Linda K. Lawrie, Frederick C. Winkelmann, W.F. Buhl, Y. Joe Huang, Curtis O. Pedersen, Richard K. Strand, Richard J. Liesen, Daniel E. Fisher, Michael J. Witte, and Jason Glazer. EnergyPlus: Creating a new-generation building energy simulation program. *Energy and Buildings*, 33(4):319–331, April 2001. ISSN 03787788. doi: 10.1016/S0378-7788(00)00114-6.
- Samuel Dodge, Jiu Xu, and Bjorn Stenger. Parsing floor plan images. In *2017 Fifteenth IAPR International Conference on Machine Vision Applications (MVA)*, pages 358–361, Nagoya, Japan, May 2017. IEEE. ISBN 978-4-901122-16-0. doi: 10.23919/MVA.2017.7986875.
- Mohamed H. Elnabawi and Neveen Hamza. A Methodology of Creating a Synthetic, Urban-Specific Weather Dataset Using a Microclimate Model for Building Energy Modelling. *Buildings*, 12(9): 1407, September 2022. ISSN 2075-5309. doi: 10.3390/buildings12091407.
- Abigail Francisco, Neda Mohammadi, and John E. Taylor. Smart City Digital Twin-Enabled Energy Management: Toward Real-Time Urban Building Energy Benchmarking. *Journal of Management in Engineering*, 36(2):04019045, March 2020. ISSN 0742-597X, 1943-5479. doi: 10.1061/(ASCE)ME.1943-5479.0000741.
- Andre Goncalves, Priyadip Ray, Braden Soper, Jennifer Stevens, Linda Coyle, and Ana Paula Sales. Generation and evaluation of synthetic patient data. *BMC Medical Research Methodology*, 20(1): 108, May 2020. ISSN 1471-2288. doi: 10.1186/s12874-020-00977-1.
- Google. ChromeDriver - WebDriver for Chrome. <https://sites.google.com/chromium.org/driver/>, June 2023. Accessed: 2025-08-06.
- Tong Guo, Max Bachmann, Mathias Kersten, and Martin Kriegel. A combined workflow to generate citywide building energy demand profiles from low-level datasets. *Sustainable Cities and Society*, 96:104694, 2023. ISSN 22106707. doi: 10.1016/j.scs.2023.104694.
- Alaeddine Hajri, Roberto Garay-Marinez, Ana M. Macarulla, and Mohamed Amin Ben Sassi. Data-driven model for heat load prediction in buildings connected to district heating networks. *Energy*, 329:136684, August 2025. ISSN 03605442. doi: 10.1016/j.energy.2025.136684.
- Sara Hooker, Dumitru Erhan, Pieter-Jan Kindermans, and Been Kim. A Benchmark for Interpretability Methods in Deep Neural Networks, November 2019.
- A Cecile J W Janssens and Forike K Martens. Reflection on modern methods: Revisiting the area under the ROC Curve. *International Journal of Epidemiology*, 49(4):1397–1403, August 2020. ISSN 0300-5771, 1464-3685. doi: 10.1093/ije/dyz274.
- Sanghyuk Lee, Jaehoon Cha, Moon Keun Kim, Kyeong Soo Kim, Van Huy Pham, and Mark Leach. Neural-Network-Based Building Energy Consumption Prediction with Training Data Generation. *Processes*, 7(10):731, October 2019. ISSN 2227-9717. doi: 10.3390/pr7100731.
- Junnan Li, Dongxu Li, Silvio Savarese, and Steven Hoi. BLIP-2: Bootstrapping Language-Image Pre-training with Frozen Image Encoders and Large Language Models, June 2023.

- Ying Lin, Yao Yao, Junlin Zhu, and Chao He. Application of Generative AI in Predictive Analysis of Urban Energy Distribution and Traffic Congestion in Smart Cities. In *2025 IEEE International Conference on Electronics, Energy Systems and Power Engineering (EESPE)*, pages 765–768, Shenyang, China, March 2025. IEEE. ISBN 979-8-3503-8957-9. doi: 10.1109/EESPE63401.2025.10987500.
- Haotian Liu, Chunyuan Li, Qingyang Wu, and Yong Jae Lee. Visual Instruction Tuning, December 2023.
- Mingzhe Liu, Liang Zhang, Jianli Chen, Wei-An Chen, Zhiyao Yang, L. James Lo, Jin Wen, and Zheng O’Neill. Large language models for building energy applications: Opportunities and challenges. *Building Simulation*, 18(2):225–234, February 2025. ISSN 1996-3599, 1996-8744. doi: 10.1007/s12273-025-1235-9.
- OpenAI. Introducing GPT-4.1 in the API. <https://openai.com/index/gpt-4-1/>, April 2025.
- Neha Patki, Roy Wedge, and Kalyan Veeramachaneni. The synthetic data vault. In *2016 IEEE International Conference on Data Science and Advanced Analytics (DSAA)*, pages 399–410, 2016. doi: 10.1109/DSAA.2016.49.
- A.T.D. Perera, Kavan Javanroodi, and Vahid M. Nik. Climate resilient interconnected infrastructure: Co-optimization of energy systems and urban morphology. *Applied Energy*, 285:116430, March 2021. ISSN 03062619. doi: 10.1016/j.apenergy.2020.116430.
- Elaina Present, Philip R. White, Chioke Harris, Rajendra Adhikari, Yingli Lou, Lixi Liu, Anthony Fontanini, Christopher Moreno, Joseph Robertson, and Jeff Maguire. Resstock 2024.1 dataset, 2024. URL <https://doi.org/10.2172/2319195>. ResStock 2024.1 dataset.
- Alec Radford, Jong Wook Kim, Chris Hallacy, Aditya Ramesh, Gabriel Goh, Sandhini Agarwal, Girish Sastry, Amanda Askell, Pamela Mishkin, Jack Clark, Gretchen Krueger, and Ilya Sutskever. Learning Transferable Visual Models From Natural Language Supervision, February 2021.
- Felix Rehmann, Martín Mosteiro-Romero, Clayton Miller, and Rita Streblov. Enhancing urban energy modeling: A case study of data acquisition, enrichment, and evaluation in Berlin. *Energy and Buildings*, 346:116070, 2025. ISSN 03787788. doi: 10.1016/j.enbuild.2025.116070.
- Nils Reimers and Iryna Gurevych. Sentence-BERT: Sentence Embeddings using Siamese BERT-Networks, August 2019.
- Janet Reyna, Anthony Fontanini, Elaina Present, Lixi Liu, Rajendra Adhikari, Carlo Bianchi, Jes Brossman, Rohit Chintala, Kenya Clark, Chioke Harris, Scott Horowitz, Yingli Lou, Jeff Maguire, Noel Merket, Nathan Moore, Prateek Munankarmi, Joseph Robertson, Noah Sandoval, Andrew Speake, Katelyn Stenger, Philip White, and Eric Wilson. Resstock technical reference documentation v3.3.0, 2025. URL <https://doi.org/10.2172/2583488>. ResStock Technical Reference Documentation.
- santoshphilip. Eppy. <https://github.com/santoshphilip/eppy>, October 2024.
- Selenium. Selenium WebDriver documentation. <https://www.selenium.dev/documentation/webdriver/>, November 2024. Accessed 2025-08-06.

- Zifan Sha, Wenwei Yue, Shuo Wang, Nan Cheng, Jiaming Wu, and Changle Li. Generative AI-Enabled Sensing and Communication Integration for Urban Air Mobility. In *2024 IEEE 99th Vehicular Technology Conference (VTC2024-Spring)*, pages 1–5, Singapore, Singapore, June 2024. IEEE. ISBN 979-8-3503-8741-4. doi: 10.1109/VTC2024-Spring62846.2024.10683276.
- Connor Shorten, Charles Pierse, Thomas Benjamin Smith, Erika Cardenas, Akanksha Sharma, John Trengrove, and Bob van Luijt. StructuredRAG: JSON Response Formatting with Large Language Models, August 2024.
- Florian Stinner, Martin Wiecek, Marc Baranski, Alexander Kümpel, and Dirk Müller. Automatic digital twin data model generation of building energy systems from piping and instrumentation diagrams, August 2021.
- The Matplotlib Development Team. Matplotlib: Visualization with Python. Zenodo, May 2025.
- U.S. Department of Energy. Getting Started. URL https://energyplus.net/assets/nrel_custom/pdfs/pdfs_v25.1.0/GettingStarted.pdf.
- U.S. Department of Energy. *EnergyPlus Auxiliary Programs Documentation — Version 23.2.0*. EnergyPlus, U.S. Department of Energy, 2023. URL https://energyplus.net/assets/nrel_custom/pdfs/pdfs_v23.2.0/AuxiliaryPrograms.pdf. See pages 45–48 for ExpandObjects preprocessor details.
- U.S. Energy Information Administration. After more than a decade of little change, U.S. electricity consumption is rising again. <https://www.eia.gov/todayinenergy/detail.php?id=65264>, May 2025.
- U.S. Environmental Protection Agency. Climate Change Indicators: Residential Energy Use. <https://www.epa.gov/climate-indicators/climate-change-indicators-residential-energy-use>, January 2025.
- Da Wan, Xiaoyu Zhao, Wanmei Lu, Pengbo Li, Xinyu Shi, and Hiroatsu Fukuda. A Deep Learning Approach toward Energy-Effective Residential Building Floor Plan Generation. *Sustainability*, 14(13):8074, July 2022. ISSN 2071-1050. doi: 10.3390/su14138074.
- Thomas Wolf, Lysandre Debut, Victor Sanh, Julien Chaumond, Clement Delangue, Anthony Moi, Pierric Cistac, Tim Rault, Remi Louf, Morgan Funtowicz, Joe Davison, Sam Shleifer, Patrick Von Platen, Clara Ma, Yacine Jernite, Julien Plu, Canwen Xu, Teven Le Scao, Sylvain Gugger, Mariama Drame, Quentin Lhoest, and Alexander Rush. Transformers: State-of-the-Art Natural Language Processing. In *Proceedings of the 2020 Conference on Empirical Methods in Natural Language Processing: System Demonstrations*, pages 38–45, Online, 2020. Association for Computational Linguistics. doi: 10.18653/v1/2020.emnlp-demos.6.
- Tong Xiao and Peng Xu. Exploring automated energy optimization with unstructured building data: A multi-agent based framework leveraging large language models. *Energy and Buildings*, 322:114691, November 2024. ISSN 03787788. doi: 10.1016/j.enbuild.2024.114691.
- Haowen Xu, Femi Omitaomu, Soheil Sabri, Sisi Zlatanova, Xiao Li, and Yongze Song. Leveraging generative AI for urban digital twins: A scoping review on the autonomous generation of urban data, scenarios, designs, and 3D city models for smart city advancement. *Urban Informatics*, 3(1):29, October 2024. ISSN 2731-6963. doi: 10.1007/s44212-024-00060-w.

- Zhengyuan Yang, Linjie Li, Kevin Lin, Jianfeng Wang, Chung-Ching Lin, Zicheng Liu, and Lijuan Wang. The Dawn of LMMS: Preliminary Explorations with GPT-4V(ision), October 2023.
- Yong Zeng, Yanpeng Cai, Guohe Huang, and Jing Dai. A Review on Optimization Modeling of Energy Systems Planning and GHG Emission Mitigation under Uncertainty. *Energies*, 4(10): 1624–1656, October 2011. ISSN 1996-1073. doi: 10.3390/en4101624.
- Liang Zhang, Vitaly Ford, Zhelun Chen, and Jianli Chen. Automatic building energy model development and debugging using large language models agentic workflow. *Energy and Buildings*, 327:115116, January 2025a. ISSN 03787788. doi: 10.1016/j.enbuild.2024.115116.
- Shaolei Zhang, Qingkai Fang, Zhe Yang, and Yang Feng. LLaVA-Mini: Efficient Image and Video Large Multimodal Models with One Vision Token, March 2025b.
- Yufei Zhang, Arno Schlüter, and Christoph Waibel. SolarGAN: Synthetic Annual Solar Irradiance Time Series on Urban Building Facades via Deep Generative Networks, June 2022.
- Deyao Zhu, Jun Chen, Xiaoqian Shen, Xiang Li, and Mohamed Elhoseiny. MiniGPT-4: Enhancing Vision-Language Understanding with Advanced Large Language Models, October 2023.
- M H Zweig and G Campbell. Receiver-operating characteristic (ROC) plots: A fundamental evaluation tool in clinical medicine. *Clinical Chemistry*, 39(4):561–577, April 1993. ISSN 0009-9147, 1530-8561. doi: 10.1093/clinchem/39.4.561.